Journal of Magnetism and Magnetic Materials 321 (2009) 1356–1363

Contents lists available at ScienceDirect

Journal of Magnetism and Magnetic Materials

journal homepage: www.elsevier.com/locate/jmmm

Preparation of biodegradable magnetic microspheres with poly(lactic acid)-coated magnetite

Hong Zhao, Katayoun Saatchi, Urs O. Häfeli *

Faculty of Pharmaceutical Sciences, University of British Columbia, 2146 East Mall, Vancouver, BC, Canada V6T 1Z3

ARTICLE INFO

Available online 20 February 2009

Keywords:
Magnetite
Coating
Stabilization
PLA
PLGA
Poly(lactic acid)
Poly (lactide-co-glycolide)
Magnetic microspheres
Biodegradability

ABSTRACT

Poly(lactic acid) (PLA)-coated magnetic nanoparticles were made using uncapped PLA with free carboxylate groups. The physical properties of these particles were compared to those of oleate-coated or oleate/sulphonate bilayer (W40) coated magnetic particles. Magnetic microspheres (MMS) with the matrix material poly(lactide-co-glycolide) (PLGA) or PLA were then formed by the emulsion solvent extraction method with encapsulation efficiencies of 40%, 83% and 96% for oleate, PLA and oleate/sulfonate-coated magnetic particles, respectively. MMS made from PLA-coated magnetite were hemocompatible and produced no hemolysis, whereas the other MMS were hemolytic above 0.3 mg/mL of blood.

0. Introduction

Functionalized biodegradable magnetic nanospheres and microspheres (MMS) are finding growing interest in a broad range of applications including targeted drug delivery, diagnostic magnetic resonance imaging (MRI), magnetic cell separation, tissue repair, hyperthermia and magnetofection [1–7]. Most of these medical applications depend on the successful synthesis of MMS made from poly(DL-lactide-co-glycolide) (PLGA) and poly(L- or DL-lactide) (PLA). These polyesters are not only biocompatible, non-toxic and biodegradable [8,9], but also FDA approved excipients and widely used in commercial sustained release products such as Lupron Depot®, Nutropin Depot®, Zoladex® and Sandostatin LAR Depot®.

The magnetic component of the MMS in general is magnetite, Fe_3O_4, a proven biocompatible iron oxide [10] which is FDA-approved and used clinically as MRI contrast agent in products such as Endorem™, Feridex®, and Resovist® [11,12]. Various procedures have been used to prepare magnetite particles, where the synthesis conditions are crucial in determining the final physicochemical properties in terms of particle size, shape, composition, and magnetic properties [13,14]. The most common synthesis of magnetite nanoparticles is based on Elmore's co-precipitation of ferrous (Fe^{2+}) and ferric (Fe^{3+}) ions under basic conditions [15] and has been perfected by Massart [16]. The overall reaction is written as follows:

$$Fe^{2+} + 2Fe^{3+} + 8OH^- \rightarrow Fe_3O_4 + 4H_2O \quad (1)$$

Thus, typically prepared 5–15 nm sized nanoparticles have a large surface-to-volume ratio and therefore high surface energies. To minimize this energy the particles tend to aggregate and form large clusters. To counteract these unwanted behaviors, different coating materials such as polyethylene glycole/polyacrylic acid (PEG/PAA) [17], starch [18], citric acid [19], oleic acid [20], decanoic acid and nonanoic acid [21] have been applied to magnetite nanoparticles to make a stable colloidal dispersion.

Magnetite-containing biodegradable PLGA or PLA microspheres have been made since the beginning of the 1990s; [22–24] however, the distribution of magnetite within the particles was rather inhomogeneous [25]. Only once coated magnetite particles were used, well-dispersed and homogeneous magnetic microspheres could be made, such as for example by Lee et al. who prepared magnetic PLGA nanoparticles with the ferrofluid W-40 [26,27]. The surface of the magnetite nanoparticles in the W-40 ferrofluid is first coated with a monolayer of sodium oleate by strong chemisorption of the carboxylic acid groups and then with a monolayer of sodium dodecylbenzenesulfonate (DBS) by weak physisorption. As an end result W-40 contains coated magnetite particles in an aqueous phase stabilized with large amounts of DBS. Although DBS by itself is not toxic, some mutagenic effects have been described in combination with ultraviolet light or other agents [28]. We were thus searching for more biocompatible coatings and thought that the polymeric matrix material themselves might be useful coatings. PLA or PLGA with carboxylate end groups are potential stabilizing coating

* Corresponding author. Tel.: 604 822 7133; fax: 604 822 3035.
E-mail address: uhafeli@interchange.ubc.ca (U.O. Häfeli).

0304-8853/$ - see front matter © 2009 Elsevier B.V. All rights reserved.
doi:10.1016/j.jmmm.2009.02.038

materials for magnetite that mix very well with the matrix material PLGA or PLA during the microsphere preparation, and are not toxic whereas sodium oleate, the currently most often used magnetite coating [29,30], should only be used in lower concentrations [21,31]. What makes the homogeneity of magnetite throughout the particle matrix very important is the planned application of these MMS for intravascular administration [1]. In this case, the MMS must be significantly smaller than red blood cells and delivered through blood vessels without clogging the smallest capillaries of 7–8 μm in diameter [32]. Also they should be as homogeneous in size as possible and contain the uniformly distributed magnetite, to achieve reliable magnetic targeting. Optimal magnetite coatings and highly compatible matrix materials are thus crucial. The aim of this study was, therefore, to prepare appropriate lipophilic magnetite particles that can be made into biodegradable MMS.

1. Methods and materials

Ferric chloride hexahydrate ($FeCl_3 \cdot 6H_2O$ >99%), ferrous chloride tetrahydrate ($FeCl_2 \cdot 4H_2O$ >99%), ammonium hydroxide (25 wt%), oleic acid (99%), methylene chloride and polyvinyl alcohol (PVA; 87–89% hydrolyzed; MW 13–23 kDa) were obtained from Sigma-Aldrich (St. Louis, MO, USA). The ferrofluid W-40 with a magnetite content of 40% was received from Taiho Industries Co. Ltd., Japan. L-Lactide was purchased from Polysciences and used without recrystallization. PLA (Resomer® L104, poly(L-lactic acid), MW 2 kDa) was purchased from Boehringer Ingelheim GmbH (Ingelheim, Germany) and PLGA (PLGA 85/15, intrinsic viscosity 0.61, MW 24 kDa) from Durect Corp. (Pelham, AL, USA). Activated partial thromboplastin time (APTT) and prothrombin time (PT) reagent kits, as well as control reagents Ci-Trol® 1 and Ci-Trol® 2 were from Dade Behring (Mississauga, ON, Canada).

Transmission electron microscopy (TEM) images were taken (Hitachi H7600, Japan) after placing a drop of MMS on a formvar-coated TEM grid (150 mesh, Ted Pella Inc. Redding, CA) and air-drying it. Scanning electron microscopy (SEM) (Hitachi S-4500, Tokyo, Japan) images were taken after sputter-coating samples with a 5 nm layer of gold–palladium. The size of magnetite nanoparticles was analyzed by a Zetasizer (Malvern Instruments, Malvern, UK). The microsphere size distribution was determined from at least 500 particles per batch from SEM images using the software ImageJ [33]. The magnetic properties of air-dried samples were determined on a vibrating sample magnetometer (VSM) (Model 155, Princeton Applied Research). Thermogravimetric analyses (TGA) were measured by heating from 20 to 550° at 20 °C/min in natural air flow (Q50, TA instrument, USA). ^1H NMR spectra were recorded on a Bruker AV-300 at 300.13. A Bruker D8 Advance X-ray diffractometer in Bragg–Brentano

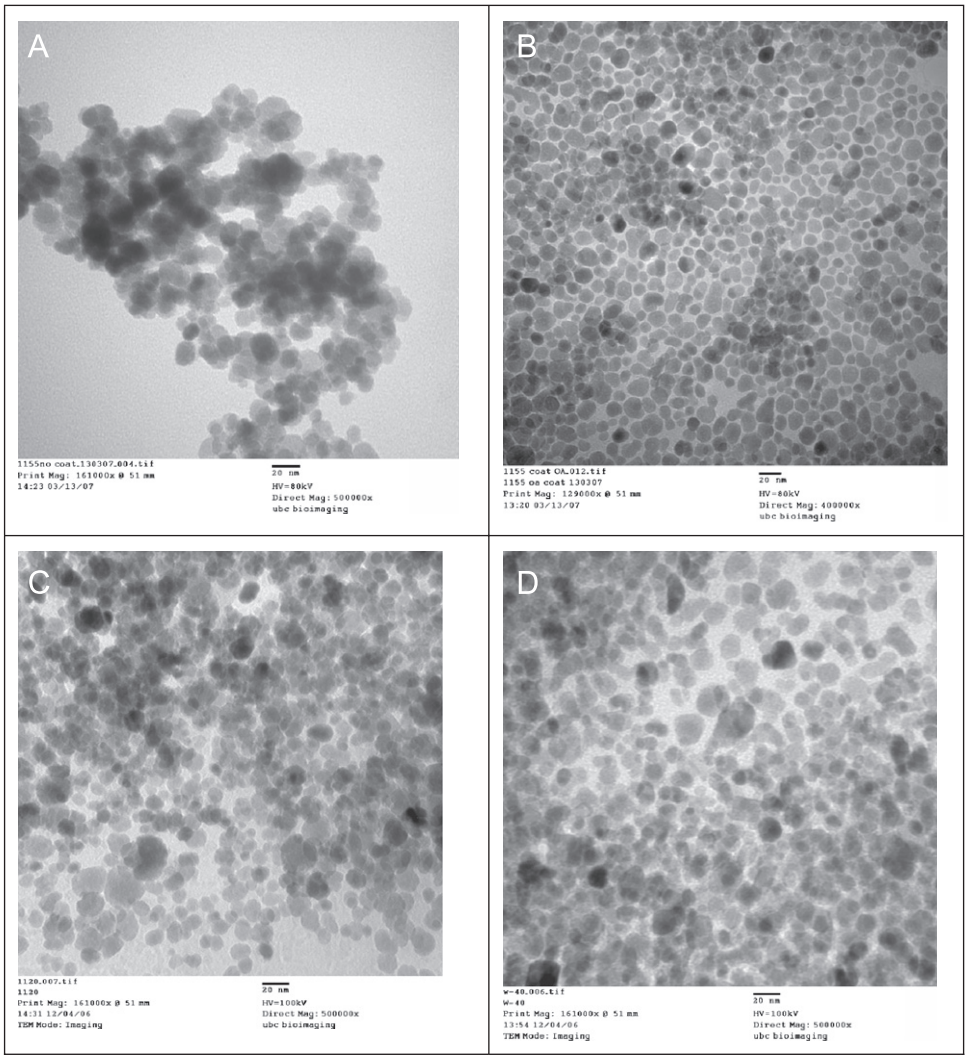

Fig. 1. TEM pictures of (A) magnetite without coating; (B) magnetite coated by oleic acid; (C) magnetite coated by PLA; and (D) ferrofluid W-40 as received.

configuration and equipped with NaI scintillation detector using Cu K_α radiation ($\lambda = 1.5406$ Å) was used. The sample holder was rotated to improve particle statistics. The generator was set at 40 kV and 40 mA. Slit sizes were set at 1.0 mm (divergence), 1.0 mm (anti-scatter), and 0.2 mm (receiving). Literature data was collected by searching PDF (Powder Diffraction Files), the intellectual property of the ICDD (International Centre for Diffraction Data).

1.1. PLA synthesis

Uncapped PLA was synthesized by ring opening polymerization of L-lactide using hydrolyzed lactide as the initiator and tin(2-ethylhexanoate) as the catalyst as reported in our previous publication [34]. ^{1}H NMR ($CDCl_3$, 300 MHz): 1.5 (d, CH_3), 5.15 (q, CH).

1.2. Preparation of PLA-coated magnetite nanoparticles

$FeCl_2 \cdot 4H_2O$ (0.6 g, 0.30 mmol) and $FeCl_3 \cdot 6H_2O$ (1.4 g, 0.52 mmol) were dissolved in 10 mL of degassed distilled H_2O and NH_4OH (2.4 mL, 29%) added with fast stirring. The flask was heated to 75 °C for 30 min and then cooled to room temperature. The particles were magnetically filtered and washed with H_2O (2–3 times). The pH of the solution was basic (9–10) before and neutral after the wash. The suspension of the particles in 5 mL water was heated to <50 °C in a closed vial for 5 min. PLA (1.4 g) dissolved in 5 mL of CH_2Cl_2 was added to this mixture with stirring. All particles moved from the aqueous to the organic phase. Water was decanted and the ferrofluid transferred to a dry vial.

1.3. Preparation of oleic-coated magnetite nanoparticles

Oleic acid-coated magnetite nanoparticles were prepared as described in the literature [29].

1.4. Preparation of PLGA and PLA microspheres

Microspheres were prepared similar to our procedure reported earlier [17]. To prepare oleic acid and PLA-coated MMS, up to a total of 250 mg of polymer and magnetite were combined into the methylene chloride phase. For the preparation of PLA-coated magnetite, the exact amount of PLA needed for further MMS preparation was used to coat the particles (i.e., the ferrofluid made was used directly to make MMS and no additional polymer was added based on 30% w/w magnetite loading). Higher loading up to 60% was attempted, however, it seemed that beyond 40% of magnetite, there was not enough PLA present to completely coat the magnetite and the particles would agglomerate. To prepare MMS containing W-40, the aqueous ferrofluid was directly added as the inner water phase to make the first w/o emulsion. The same protocol described above was then followed.

1.5. APTT and PT hemocompatibility tests

The hemocompatibility of different coating materials and MMS was tested by *in vitro* hemolysis using the activated partial thromboplastin time and prothrombin time tests with a coagulation analyzer using mechanical end point determination (ST4, Diagnostica Stago). Plasma from healthy volunteers was separated by centrifugation of whole blood at 117 g for 12 min and used within 12 h. All test samples were used at a concentration of 7.5 mg/mL in phosphate-buffered saline (PBS) pH 7.4. For the APTT determination the intrinsic and common coagulation pathways were activated by adding actin (a partial thromboplastin reagent) and calcium chloride to plasma and measuring the clotting time. First, plasma (100 μL), sample solution (100 μL) and actin (200 μL) were mixed, then 100 μL of the above mixture pipetted to a cuvette, incubated at 37 °C for 3 min, and then 50 μL of 0.025 M $CaCl_2$ was added. The time for initiation of clot formation was measured and recorded. For the PT determination, the extrinsic and common coagulation pathways were activated by incubating plasma with the innovin reagent and measuring the clotting time. Generally, 50 μL of a mixture of plasma (100 μL) and sample solution (100 μL) were pipetted into cuvette wells and incubated at 37 °C for 60 s. To each well, 100 μL of innovin was added and time to coagulation determined as above. Control experiments were done adding identical volumes of PBS and Ci-Trol® 2 (abnormal plasma control). Each experiment was repeated four times.

1.6. Hemolysis assay

Fresh blood was collected from healthy volunteers into heparin containing vacutainer tubes (VWR Scientific, Mississauga, ON). Erythrocytes were then separated by centrifugation (12 min at 117 g), washed with PBS (3 ×), diluted and resuspended to give a final concentration of around 2×10^8 erythrocytes per ml in PBS, as counted by hemocytometer. A 0.5 mL sample solution (15 mg/mL) in PBS was then added to 0.5 mL of erythrocyte solution and incubated at 37 °C for 1.5, 3 and 5 h, at that time blood cells and sample precipitates were sedimented in a centrifuge (10 min at 11,752 g). The release of hemoglobin from the erythrocyte cells was measured spectrophotometrically at 540 nm in the supernatant (8452 A diode array spectrophotometer, Hewlett Packard, Kirkland, PQ). All trials were run three times. Results were expressed as a percentage of the total efflux of hemoglobin obtained by adding 0.5 mL of 2% Triton X-100 to 0.5 mL of erythrocyte solution. A spontaneous hemolysis control group was determined by incubating erythrocytes at 1×10^8 cells/mL in PBS alone.

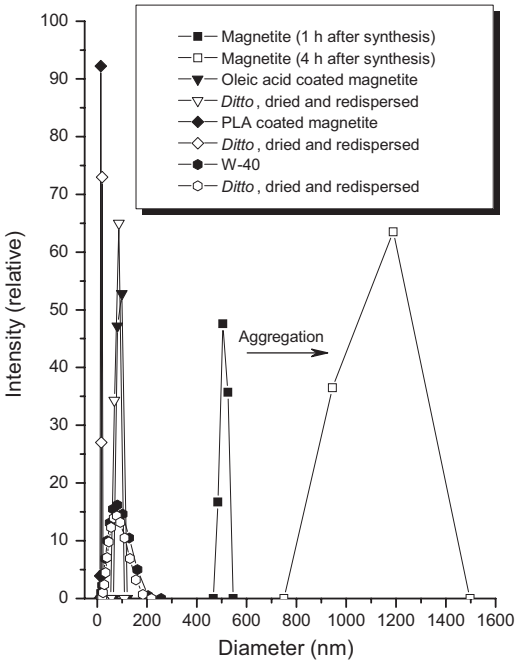

Fig. 2. Size and stability of magnetite without coating, oleic acid coated, PLA coated and of W-40 ferrofluid.

2. Results and discussion

Uncapped PLA was successfully used to coat magnetite particles, which made them lipophilic and readily dispersable in organic solvents such as CH_2Cl_2. Using of commercial PLA (e.g., Resomer L104) did not provide a suitable coating for the magnetic particles as PLA is usually capped (esterified with short carbon chains) to increase the shelf life of the polymer. TEM images of magnetite nanoparticles (Fig. 1) showed that all the tested coating materials were able to separate the single-magnetite crystals from each other (Fig. 1B–D). Uncoated magnetite, however, agglomerated due to their high surface

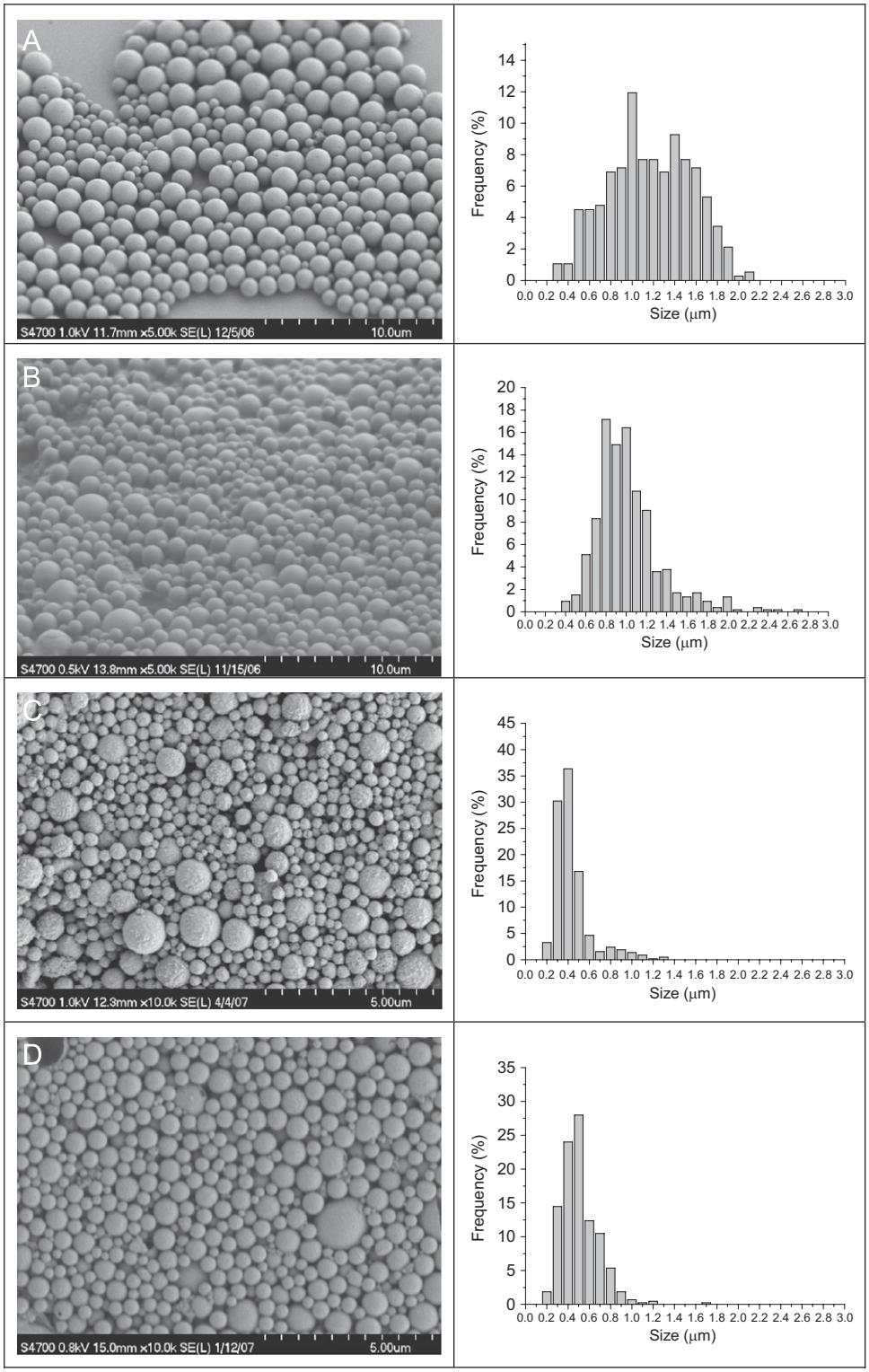

Fig. 3. SEM pictures of microspheres (on the left) and their corresponding size distribution (on the right). (A) PLGA microspheres; (B) PLA-coated MMS, 28.81% magnetite loading; (C) W-40-formulated PLGA MMS, 51.20% magnetite loading; and (D) oleic acid-coated PLGA MMS, 20.84% magnetite loading.

energy of the nanoparticles (Fig. 1A). The measurement of the particles' size distribution (Fig. 2) confirmed these observations. Without a coating agent, magnetite nanoparticles clumped together, and grew within 4 h to agglomerates of more than 1 μm in size. Such agglomerates cannot be dispersed anymore, not even by ultrasound treatment. For all 3 types of the coated nanoparticles, however, even drying and redispersion several weeks later resulted in unaltered size distributions and thus good size stability (Fig. 2).

As shown experimentally, uncoated magnetite nanoparticles have a large surface area-to-volume ratio, which gives them the tendency to increase in particle size due to agglomeration and large cluster formation, which in turn can show strong magnetic dipole–dipole attraction and ferromagnetic behavior [35]. For effective stabilization of iron oxide nanoparticles, a high coating density is thus desirable. Potential stabilizing agents include polymers (e.g., PEG/PAA [17]), various long-chain carboxylic acids, phosphonates and phosphates [36]. Alkyl phosphonates and phosphates yield more thermodynamically stable dispersions of magnetite nanoparticles than oleic acid at physiological pH and might thus be preferred [36].

The preparation of MMS with native and coated magnetite by double emulsion–solvent extraction yielded MMS of around 1 μm in size, as shown by SEM pictures and corresponding size distributions (Fig. 3). All MMS were spherical, and with the exception of the W-40 formulated ones (Fig. 3C), they all showed smooth surfaces.

2.1. Characteristics of iron oxide nanoparticles and MMS

While the organic substances, oleic acid and PLA showed a complete weight loss in TGA in a single step when being heated from 25 to 550 °C (Fig. 4A and C), native magnetite showed an overall weight gain of 2.576% (Fig. 4B). In addition, the color of the material changed from black to red that was due to complete oxidation of magnetite according to the overall scheme of

$$2Fe_3O_4 + 0.5O_2 \rightarrow 3Fe_2O_3 \quad (2)$$

Theoretically, the molecular weight should have increased by 3.455%. The difference between the observed and theoretical weight increment was likely due to the original starting sample consisting not only of magnetite, but also some maghemite (γ-Fe_2O_3). A mixture of 74.56% magnetite and 25.44% of maghemite in the original sample would lead to a calculated 2.576% of weight increment. An analysis of the original sample by X-ray diffraction before and after TGA (Fig. 5) revealed this hypothesis to be very likely. The major diffraction peaks could be assigned to related reflection lines and were in good agreement with the literature values for magnetite [37] (PDF#01-089-0691), maghemite [38] (PDF#01-089-5892) and hematite [39] (PDF#01-089-0596). Initially, the diffraction pattern of the particles showed the characteristics of magnetite or maghemite—it is impossible to separate the two based only on their diffraction pattern. After TGA in air, however, there was a

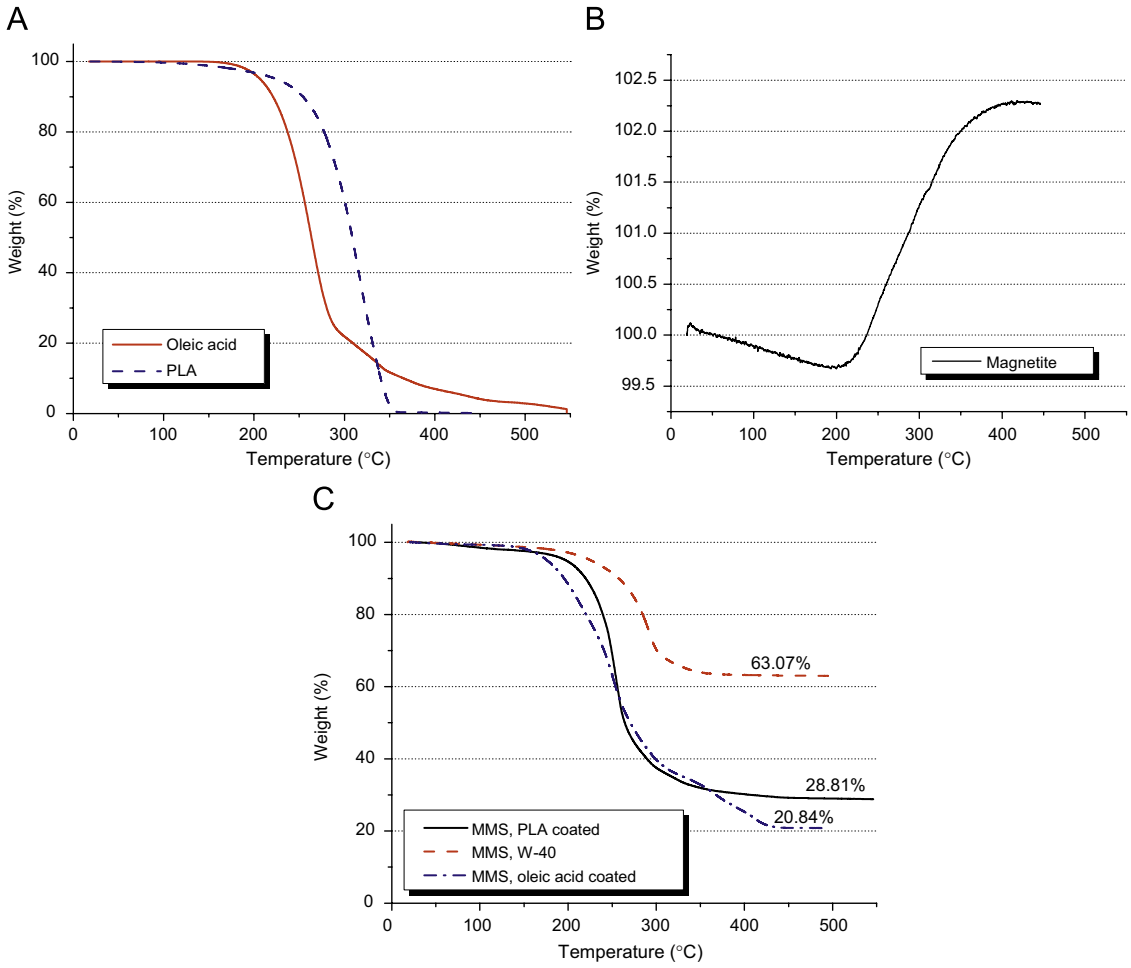

Fig. 4. TGA results. (A) Oleic acid and PLA; (B) magnetite; and (C) PLA-coated MMS (28.81% magnetite loading); oleic acid-coated MMS (20.84% magnetite loading); W-40-formulated MMS (63.07% magnetite loading).

clear transformation of magnetite to hematite (α-Fe_2O_3), as has been reported before [40].

Based on TGA, the final iron oxide content of the MMS was 20.84% for oleic acid-coated MMS, 28.81% for PLA-coated MMS and 63.07% for the W-40 ferrofluid encapsulated MMS batches, respectively. The calculated encapsulation efficiencies were thus 40%, 83% and 96%, respectively. Encapsulating magnetite from the inner water phase yielded the highest loading efficiencies.

All MMS exhibited the typical superparamagnetic behavior of zero coercivity and no remanence in their magnetization curves measured at room temperature (Fig. 6). This was even true for the native, uncoated magnetite, whose aggregate size was above 1000 nm (Fig. 1B). The aggregates, thus, still consist of single particles with a saturation magnetization of 58.5 emu/g. MMS loaded with 63.07% iron oxide from W-40 exhibited a saturation magnetization of 37.8 emu/g. MMS loaded with 28.81% iron oxide coated by PLA showed a magnetization of 19.2 emu/g, while MMS loaded with 20.84% magnetite coated by oleic acid showed one of 12.9 emu/g. The measured saturation magnetizations are within 5.5% of the theoretical values expected from the TGA measurements.

2.2. APTT and PT determination

For *in vivo* clinical applications the MMS will be in contact with blood; therefore, their effect on the induction of (unwanted) blood clotting had to be investigated. The blood coagulation cascade includes intrinsic and extrinsic pathways that were evaluated by APTT and PT studies, respectively. As shown by the white bars in Fig. 7, none of the MMS or control substances prolonged the time until normal fibrin clot formation with the PT assay. The extrinsic pathway of coagulation is thus not affected at all by MMS and coating materials. The evaluation of the intrinsic pathway by APTT, however, showed that some samples prolonged bleeding times (grey bars in Fig. 7). Compared to the PBS control, PLA-coated magnetite microspheres, oleic acid-coated magnetite microspheres and W-40 prolonged APTT significantly ($P<0.001$), although none of the values reached the intermediate elevated (abnormal) range of the Dade Ci-Trol® coagulation control (Fig. 7). Many foreign materials show such a change of plasma coagulation properties, as for example different polymers [41], hydrogels [42] and Nitinol devices [43]. Changes in coagulation properties might lead to thrombosis, although at least one paper describes that using APTT results should only be used as an indication of biomaterial induced coagulation activity, not as absolute results [41]. Some studies have concluded that activation of contact system started by interaction of negative-charged surfaces with plasma [44]. The possible presence of carboxylate groups at the

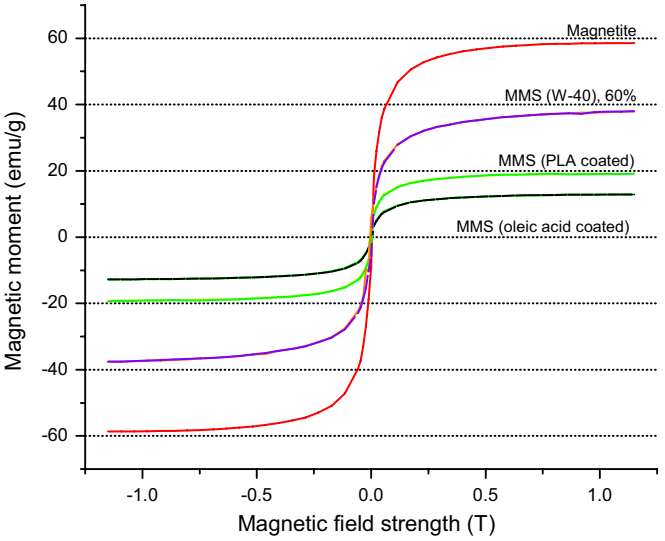

Fig. 6. Vibrating sample magnetometer (VSM) results of different MMS.

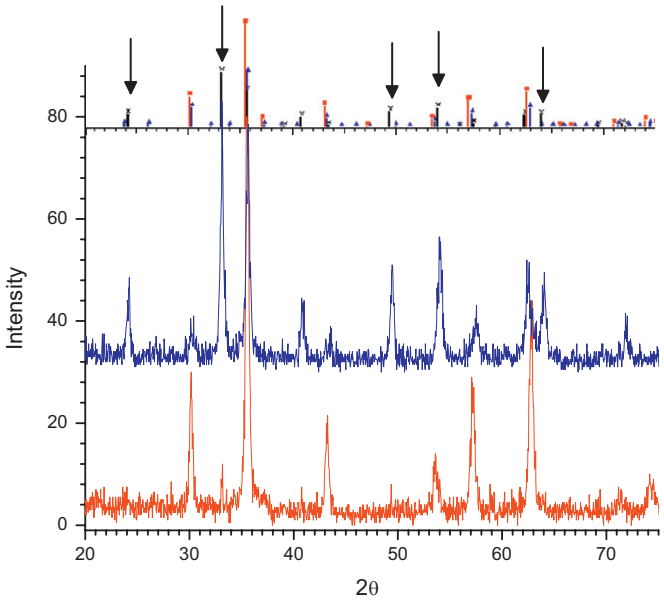

Fig. 5. Powder X-ray diffraction spectra of PLA-coated particles before (bottom) and after (middle) TGA along with references (top) for magnetite (■), maghemite (▲), and hematite (×). The arrows show appearance of new signals characteristic of hematite.

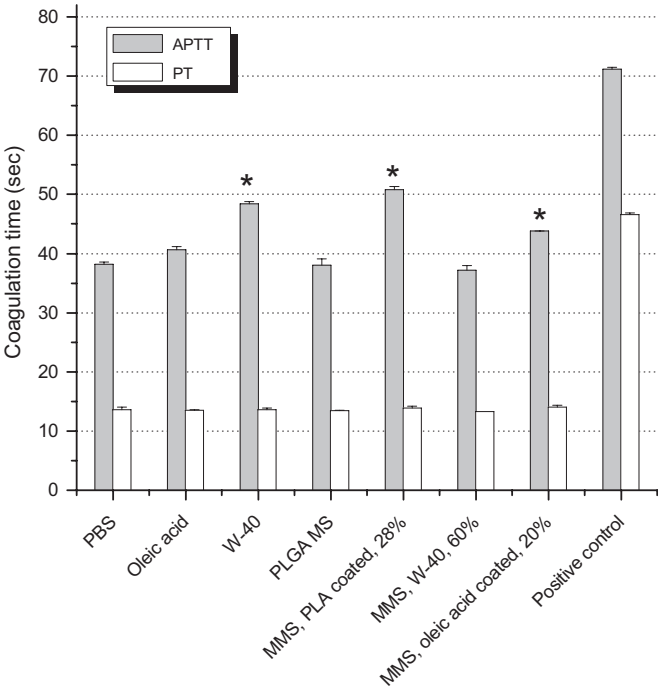

Fig. 7. APTT and PT hemocompatibility results. The positive control is the intermediate elevated (abnormal) range of the Dade Ci-Trol® coagulation control agent. * $P<0.001$.

PLA MMS surface, which at physiological pH would be negatively charged, might be the reason behind prolonged APTT times. If necessary, this could be prevented by optimizing the amount of carboxylated PLA during magnetite coating and adding capped PLA as matrix material during the MMS preparation.

2.3. *In vitro hemolysis analysis*

Any substances to be used in parenteral formulations must be tested for potential incompatibility with red blood cells [45]. The most often used method to investigate the erythrocyte membrane-damaging properties of polymers is the *in vitro* hemolysis assay [46], where the release of hemoglobin is quantified. In the current study, empty PLGA microspheres and PLA-coated MMS produced less than 10% hemolysis at all tested concentrations up to 7.5 mg/mL (Fig. 8A and B). PLA-coated magnetite MMS are thus compatible with erythrocytes. Furthermore, it seems that the PLA coating adds a protective effect from hemolysis, since hemolysis of magnetite nanoparticles at an iron concentration of 0.1 M, which is similar to the highest tested

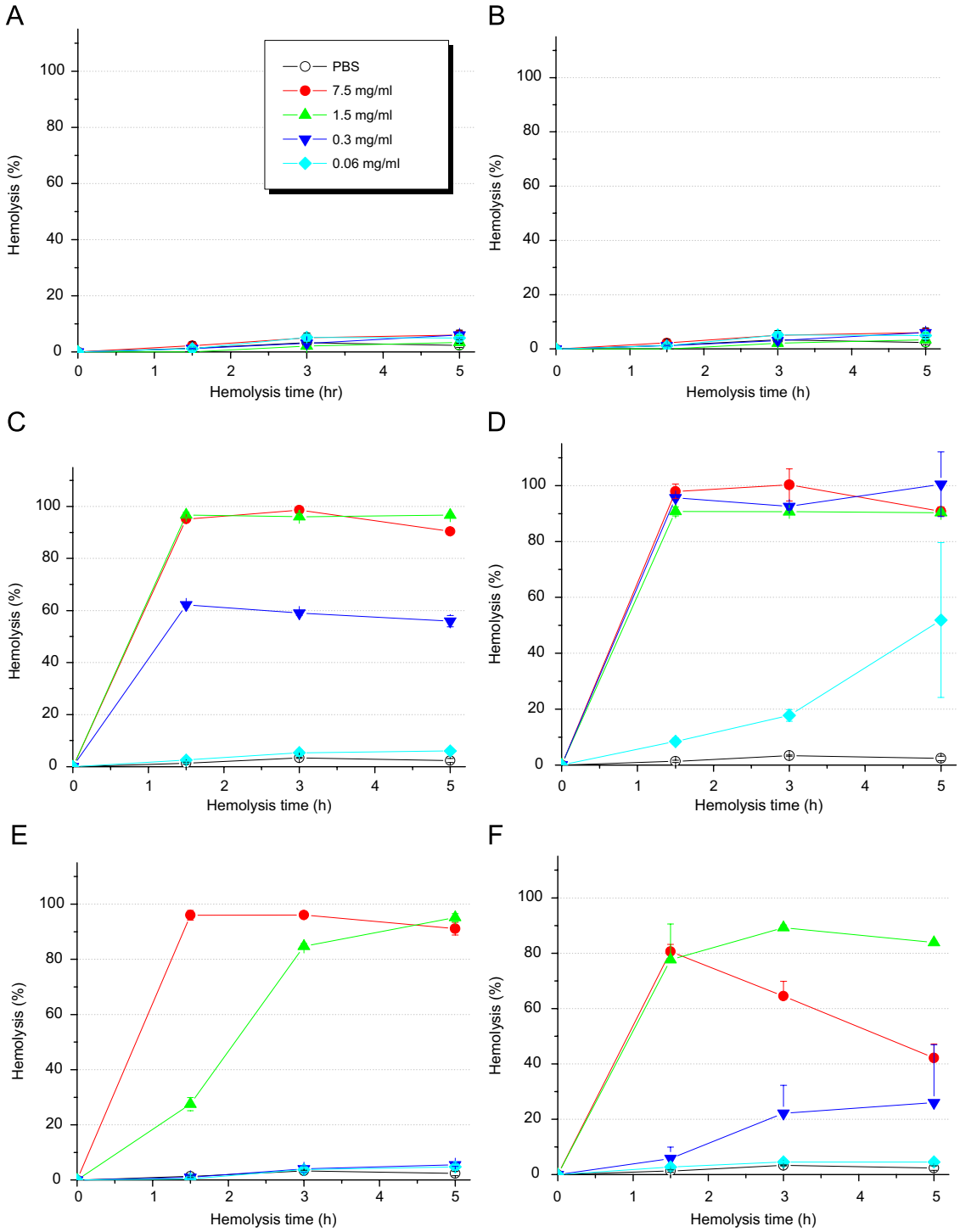

Fig. 8. Hemolysis caused by different materials. (A) PLGA MS; (B) PLA-coated MMS; (C) W-40 ferrofluid; (D) oleic acid; (E) W-40-formulated MMS; (F) oleic acid-coated MMS. ●7.5 mg/mL; ▲1.5 mg/mL; ▼0.3 mg/mL; ◆0.06 mg/mL; ○PBS.

concentration here, has been reported to be significant [47]. The other test samples, W-40 ferrofluid and oleic acid-coated magnetic particles induced hemolysis of erythrocytes at concentrations as low as 0.3 and 0.06 mg/mL, whereas hemolysis was complete (100%) at 1.5 mg/mL for W-40 and 0.3 mg/mL for oleic acid (Fig. 8C and D).

Hemolysis is both concentration and time dependent, as shown in Fig. 8E and F. W-40 MMS used in concentrations of 0.3 mg/mL or oleic acid-coated MMS in concentrations of less than 0.06 mg/mL are hemocompatible (less than 5% hemolysis), while higher concentrations lead to hemolysis, very likely due to the nature of coating and the stabilizer's surfactant activity. It is therefore appropriate for *in vivo* applications to early add-on hemocompatibility studies to other toxicity studies such as the MTT assay.

Despite these findings, oleic acid is widely used as a stabilizer or coating material for magnetite nanoparticles [20,29,48], designed for *in vivo* targeted delivery applications after vascular injection [49]. In general, oleic acid has been considered a relatively non-toxic coating material. Magnetite nanoparticles coated by oleic acid at total blood volume concentrations of 4% in rats, however, showed significant side effects, such as diarrhea, tachycardia, tachypnea, seizure, crowing position, clonic convulsion and immediate shock [21].

W-40 ferrofluids with low loading concentrations of about 5% have been encapsulated in nanoparticles [26,27] and successfully used as an MRI contrast agent in the kidney of rabbits [27]. Oleic acid and sodium dodecylbenzenesulfonate used as magnetite stabilizers can thus induce significant hemolysis even at rather low concentrations. MMS made from magnetite nanoparticles coated with these materials can produce hemolytic effects, which might be a serious barrier for further *in vivo* applications. Hemocompatibility tests of MMS should thus be a part of the biocompatibility testing of microspheres early on. Although APTT, PT and hemolysis tests may give a good indication of potential toxicity, only the actual clinical evaluation will be able to pinpoint the relevance and importance of these findings.

Therefore, use of uncapped PLA as a coating material for magnetite in order to make biodegradable MMS serves a dual purpose. It can not only be used as the matrix material for the preparation of MMS; but also as a lipophilic stabilizer. Its known biocompatibility has been confirmed, and its hemocompatibility is excellent at all tested concentrations. The highest concentration of 7.5 mg/mL was chosen to be appropriate for clinical drug delivery applications. From our results, both PLA and PLGA showed excellent hemocompatibility with red blood cells. Therefore, similarly-uncapped PLGA can be used to coat the magnetic particles. Important for the use of both polymers is the fact that they have free carboxylate groups. Most commercially available polymers are capped at both ends to increase shelf life of the material, and are not useful for magnetite coating as there is no anchoring possible to the surface of the magnetite.

Acknowledgements

Kelly Gilmour is acknowledged for the magnetic measurements. We appreciate funding by the Canadian Institutes of Health Research (CIHR) Grant MOP-74597 and the Natural Sciences and Engineering Research Council of Canada (NSERC) discovery grant.

References

[1] U.O. Häfeli, in: R. Arshady, K. Kono (Eds.), Smart Nanoparticles in Nanomedicine—the MML Series, Vol. 8, Kentus Books, London, UK, 2006, p. 77.
[2] I. Hilger, F. Hofmann, J.R. Reichenbach, et al., Rofo. Fortschr. Geb. Rontgenstr. Neuen Bildgeb. Verfahr. 174 (2002) 101.
[3] Z. Berkova, J. Kriz, P. Girman, et al., Transplant. Proc. 37 (2005) 3496.
[4] L.L. Muldoon, M. Sandor, K.E. Pinkston, et al., Neurosurgery 57 (2005) 785.
[5] M. Radisic, R.K. Iyer, S.M. Murthy, Int. J. Nanomed. 1 (2006) 3.
[6] D.C.F. Chan, D.B. Kirpotin, P.A. Bunn, J. Magn. Magn. Mater. 122 (1993) 374.
[7] C. Plank, F. Scherer, U. Schillinger, et al., J. Liposome Res. 13 (2003) 29.
[8] C.C. Chu, in: D.F. Williams (Ed.), CRC Critical Reviews in Biocompatibility, Vol. 1, CRC Press, Boca Raton, 1985, p. 261.
[9] J.L. Cleland, in: Sanders, Hendren (Eds.), Protein Delivery: Physical Systems, Plenum Press, New York, 1997, p. 1.
[10] U. Schwertmann, R.M. Cornell, Iron Oxides in the Laboratory: Preparation and Characterization, first ed., Weinheim, New York, 1991.
[11] Y.X. Wang, S.M. Hussain, G.P. Krestin, Eur. Radiol. 11 (2001) 2319.
[12] L.X. Tiefenauer, in: T. Vo-Dinh (Ed.), Nanotechnology in Biology and Medicine: Methods, Devices, and Applications, Vol. Section D Nanomedicine Applications D1, CRC Press, Taylor and Francis, Boca Raton, FL, USA, 2007, p. 1.
[13] Y. Sahoo, A. Goodarzi, M.T. Swihart, et al., J. Phys. Chem. B Condens. Matter Mater. Surf. Interfaces Biophys. 109 (2005) 3879.
[14] J. Park, E. Lee, N.M. Hwang, et al., Angew. Chem. Int. Ed. Engl. 44 (2005) 2872.
[15] W.C. Elmore, Phys. Rev. 54 (1938) 309.
[16] R. Massart, Patent no. 4,329,241 (US), May 11.
[17] H. Zhao, J. Gagnon, U.O. Häfeli, Biomagn. Res. Technol. 5 (2007) 2.
[18] S. Levine, Science 123 (1956) 185.
[19] N. Fauconnier, A. Bee, J. Roger, et al., Prog. Colloid Polym. Sci. 100 (1996) 212.
[20] Z. Wang, H. Guo, Y. Yu, et al., J. Magn. Magn. Mater. 302 (2006) 397.
[21] S.I. Park, J.H. Lim, J.H. Kim, et al., Phys. Status Solidi (b) 241 (2004) 1662.
[22] D.G. Duguay, Ph.D. Thesis, McGill, 1991.
[23] I.J. Oh, J.Y. Oh, K.C. Lee, Arch. Pharm. Res. 16 (1993) 312.
[24] U.O. Häfeli, S.M. Sweeney, B.S. Beresford, et al., J. Biomed. Mater. Res. 28 (1994) 901.
[25] S.K. Kraeft, U.O. Häfeli, L.B. Chen, in: U. Häfeli, W. Schütt, J. Teller, et al. (Eds.), Scientific and Clinical Applications of Magnetic Carriers, Plenum, New York, 1997, p. 149.
[26] S.J. Lee, J.R. Jeong, S.C. Shin, et al., Colloids Surfaces A: Physicochemical Eng. Aspects 255 (2005) 19.
[27] S.J. Lee, J.R. Jeong, S.C. Shin, et al., J. Magn. Magn. Mater. 272–276 (2004) 2432.
[28] K. Murakami, T. Kinouchi, H. Matsumoto, et al., Tokushima J. Exp. Med. 43 (1996) 47.
[29] X. Liu, M.D. Kaminski, Y. Guan, et al., J. Magn. Magn. Mater. 306 (2006) 248.
[30] M.A. Morales, T.K. Jain, V. Labhasetwar, et al., J. Appl. Phys. 97 (2005) 10Q905.
[31] J. Sun, S. Zhou, P. Hou, et al., J. Biomed. Mater. Res. A 80 (2007) 333.
[32] Y.C. Fung, Biomechanics: Circulation, second ed., Springer, New York, 1997.
[33] M.D. Abramoff, P.J. Magelhaes, S.J. Ram, Biophotonics Int. 7 (2004) 36.
[34] K. Saatchi, U.O. Häfeli, Dalton Trans. 39 (2007) 4439.
[35] A.K. Gupta, M. Gupta, Biomaterials 26 (2005) 3995.
[36] Y. Sahoo, H. Pizem, T. Fried, et al., Langmuir 17 (2001) 7907.
[37] H. Fjellvag, F. Gronvold, S. Stolen, et al., J. Solid State Chem. 124 (1996) 52.
[38] H.-S. Shin, Yoop Hakhoechi 35 (1998) 1113.
[39] V.A. Sadykov, L.A. Isupova, S.V. Tsybulya, et al., J. Solid State Chem. 123 (1996) 191.
[40] R.M. Cornell, U. Schwertmann, The Iron Oxides: Structure, Properties, Reactions, Occurrences and Uses, VCH, Weinheim, 1996.
[41] R.K. Kainthan, S.R. Hester, E. Levin, et al., Biomaterials 28 (2007) 4581.
[42] L.P. Amarnath, A. Srinivas, A. Ramamurthi, Biomaterials 27 (2006) 1416.
[43] X. Kong, R.G. Grabitza, W.V. Oeverenb, et al., Biomaterials 23 (2002) 1775.
[44] A.P. Kaplan, M. Silverberg, Blood 70 (1987) 1.
[45] D. Shim, D.S. Wechsler, T.R. Lloyd, et al., Cathet. Cardiovasc. Diagn. 39 (2007) 287.
[46] D. Fischer, Y. Li, B. Ahlemeyer, et al., Biomaterials 24 (2003) 1121.
[47] F.Y. Cheng, C.H. Su, Y.S. Yang, et al., Biomaterials 26 (2005) 729.
[48] V.V. Korolev, A.G. Ramazanova, A.V. Blinov, Russ. Chem. Bull. 51 (2002) 2044.
[49] X.Q. Liu, M.D. Kaminski, J.S. Riffle, et al., J. Magn. Magn. Mater. 311 (2007) 84.